PERGAMON

Electrochimica Acta 45 (1999) 659–673

ELECTROCHIMICA Acta

www.elsevier.nl/locate/electacta

Quantum and simulation studies of $X^-(H_2O)_n$ systems

Anna Ignaczak [a], J.A.N.F. Gomes [b,*], M.N.D.S. Cordeiro [b]

[a] *Department of Theoretical Chemistry, University of Lodz, ul. Pomorska 149/153, 90-236 Lodz, Poland*
[b] *CEQUP/Faculdade de Ciências, Universidade do Porto Rua do Campo Alegre 687, 4150 Porto, Portugal*

Received 26 September 1998; received in revised form 1 January 1999

Abstract

This paper reports on studies of the interactions of halide ions with water. The standard Hartree–Fock (HF) method was used to calculate the interaction between each of the four halide ions and the water monomer. The structural properties of the X^-–H_2O systems (X=F, Cl, Br, I) are presented with a detailed comparison with experimental energies. A new ion–water parameterised potential, derived from quantum calculations, is proposed for the description of the X^-–H_2O interactions in simulations. This potential was used in Monte Carlo (MC) studies of the gas-phase formation of $X^-(H_2O)_n$ clusters ($n = 1, \ldots, 10$) and of the solvation of the ions in dilute aqueous solutions. Thermodynamic properties, such as enthalpies, $\Delta H_{n-1,n}$, Gibbs free energies, $\Delta G_{n-1,n}$, and entropies, $\Delta S_{n-1,n}$, are presented for the gas-phase reactions: $X^-(H_2O)_n + H_2O \rightleftharpoons X^-(H_2O)_n$. The results follow the general experimental trends, but overestimate their absolute values for the smaller clusters. The structural properties of the small clusters were found to be in good agreement with the results of quantum calculations. For small n, the so-called surface (S) structure was found to be predominant, while for larger n the interior (I) structure is preferred. The transition from an (S) structure to an (I) structure was found to occur for n between 4 and 6, depending on the ion. In solution, the energy of solvation and the structural properties of each ion are reported and compared with the experimental data available. The energy values were found to be in good agreement with estimates reported for the three larger ions, while for fluoride they are slightly overestimated. © 1999 Elsevier Science Ltd. All rights reserved.

Keywords: Hydration of halide ions; Quantum calculations; Monte Carlo simulations

1. Introduction

The properties of the $X^-(H_2O)_n$ systems (where X=F, Cl, Br, I) have been the subject of many theoretical investigations in the past. In several works the interaction of halide ions with a single water molecule was studied by quantum calculations [1–11]. The microscopic features of the solvation of anions in water clusters were analysed by quantum [1–11] as well as by simulation [12–28] techniques. The structural and thermodynamic properties of the halide ions in bulk water were widely investigated using simulation methods [29–45]. It can be said that, in general, the results reported exhibit a strong dependency on the methods used. In the case of the quantum studies, the results obtained depend on the choice of the basis set used to describe the ion and the water molecule as well as on the choice of the computational technique used. In simulations, the choice of the potentials used for the description of the interactions of the systems, as well as some other initial assumptions is known to strongly affect the final results.

For example, in the Hartree–Fock (HF) studies of Del Bene [1] the ion–water binding energy has been found to be -114 kJ mol^{-1} for the fluoride–water dimer and -54 kJ mol^{-1} for the chloride–water system. In the work of Combariza et al. [4] the values of

---

* Corresponding author. Fax: +351-2608-2959.
E-mail address: jfgomes@fc.up.pt (J.A.N.F. Gomes)

0013-4686/99/$ - see front matter
PII: S0013-4686(99)00245-5

-54 kJ mol^{-1} for chloride, -46 kJ mol^{-1} for bromide and -39 kJ mol^{-1} for iodide have been reported from calculations at the MP2 level. The relatively weak interaction of fluoride with a water molecule (-87 kJ mol^{-1}) has been found in the work of Zhan et al. [9] from MP4 calculations. Combariza et al. [10] has very recently obtained a much stronger value (-120 kJ mol^{-1}) for this ion, based on DFT calculations. A very wide range of energy values was found in the work of Kuznetsov [6], where the interaction of the four halide ions with the water molecule has been studied using ab initio methods. The X^-–H_2O energies of -101 to -164 kJ mol^{-1} for F^-, of -52 to -88 kJ mol^{-1} for Cl^-, of -54 to -68 kJ mol^{-1} for Br^- and of -40 to -49 kJ mol^{-1} for I^-, have been reported in this latter work. These extremely different results were obtained by only changing the basis sets used for the ion–water system.

As mentioned above, a comparison of results obtained for halide ions in aqueous solution and in small clusters, clearly shows that the properties found from theoretical studies depend strongly on the method and potentials used. The structural and energetic properties of small $X^-(H_2O)_n$ clusters were found to differ significantly when they were investigated by quantum methods and simulation techniques. In the latter case, the results seem to be determined by the ion–water and water–water potentials used in simulations. Most frequently, the ion–water potentials used in the simulations are pairwise additive potentials derived from the results of quantum calculations, however some attempts to include many-body effects have been also made [23–28,31,39]. The thermodynamic properties of the gas-phase formation of these small clusters were found to be very sensitive in simulations to the type of potential used for the description of the ion–water and water–water interactions. The importance of the many-body effects in these systems needs to be stressed [23–28].

The properties of halides in liquid solution, reported from Monte Carlo (MC) [29–34] and Molecular Dynamics (MD) [35–45] studies, have also been found to depend on the model used. The coordination number, the geometrical features of the first hydration shell and the solvation energy differ significantly when results obtained with different methods are compared. At the same time, some additional difficulty appears in the verification of the computed values by comparing them with those obtained from experimental measurements in gas-phase [46–54] and in aqueous solution [55–63]. The wide range of values reported for the same property seems to indicate that experimental studies also have a relatively large margin of uncertainty.

In theoretical studies of aqueous solutions of X^- ions one must make some initial assumption about the X^-–H_2O dimer. In this work, to avoid the ambiguity due to the basis set dependency of the results, quantum calculations have been performed with the goal of obtaining the best reconstruction of the optimal energy values reported from experiment. In Section 2, the results of tests performed for several different basis sets for the optimised ion–water conformations are presented and compared with experimental data. Some additional information about the X^-–H_2O (X=F, Cl, Br, I) systems, not available from experiment, is also shown.

The basis sets which best reproduce the experimental data while keeping an affordable computational cost were used for the construction of potential energy surfaces for each ion. These surfaces were then used for fitting an analytical pairwise additive potential proposed, in Section 3, for the description of the ion–water interactions in the simulations. However, it should be stressed that these simulations are based on HF calculations and on simple basis sets, a strategy that may take advantage of cancelling effects.

The results of systematic studies on the properties of halide ions in gas-phase water clusters and in liquid water are presented in Sections 4 and 5, respectively. These properties were studied by the MC method. For the small clusters, the structural and the thermodynamic properties, such as free energy of formation and enthalpy, have been computed and compared with experimental values. For the liquid phase the structural properties of the aqueous environment of the ions have been characterised through radial distribution functions (RDFs). The hydration energy for each ion in solution has also been computed and results are compared with theoretical and experimental data available.

This work is part of more extended studies performed by the authors on the specific adsorption of ions on metals [64–66]. This interesting electrochemical phenomenon has been widely investigated in the past, using quantum ([64,65] and Refs. therein) and statistical ([66] and Refs. therein) methods. In the process of specific adsorption, one of the most important phenomena is the modification of the hydration environment of the ion (and metal) when it approaches the surface. It is believed that the results of the present paper, in conjunction with those reported in Ref. [66], allow for a better analysis and understanding of the theoretical results already reported for the interfacial region.

2. Ion–water quantum calculations

2.1. (a) Method

The interaction energies of the halide ions with the water monomer were carried out at the standard HF level. The basis sets used for the halide ions were the following: for the three larger ions, Cl^-, Br^- and I^-, the inner shells were described by the effective-core potentials (ECPs) of Hay and Wadt [67] and their valence electrons by the double-zeta quality basis set developed by the same authors; for fluoride, the all-electron double-zeta quality basis set of Dunning/Huzinaga [68] has been used. It should be noticed that these basis sets were the same as those used in the studies of the specific adsorption of ions on metal surfaces [64,65].

The H_2O molecule was kept rigid at its experimental geometry, i.e. with a H–O–H angle of 104.52° and O–H distances of 0.9572 Å. Several different basis sets for the water molecule (with different polarisation functions, including *f* functions and diffuse functions) were tested to obtain interaction energies for the ion–water dimers as close as possible to the experimentally known data. In the present work, results are shown only for the (A) 6-31G* basis set [69,70], the (B) 6-31G(2D) and the (C) 6-31G(3D) basis sets [69,71], these giving the best estimates. For each case, the water–oxygen distance, r, and the tilt angle, α, between the dipole moment of the water and the ion–oxygen vector (see Fig. 1) have been optimised. The basis set superposition error (BSSE) was calculated using the counterpoise (CP) method [72]. All calculations were performed using the Gaussian92 and Gaussian98 programs [73].

Here, it should be remarked that the reason for not using a 6-31 G* type of basis set for all the ions and the water molecule was based on the results of Kuznetsov [6], as the dimer energies become overestimated. For the smaller ions, some additional tests were performed using the 6-31G basis sets with polarisation and diffuse functions for both ion and water, namely the 6-31 G**, the 6-31 + G** and the 6-31 + + G** basis sets [69–71]. Nevertheless, the results obtained always gave overestimated energies for F^- and either overestimated or underestimated energies for Cl^- and Br^-, sometimes showing strange behaviour. For example, when the 6-31 G** basis set was used, for both ions and the water molecule, the energy values obtained are equal to −58.5 kJ mol^{-1} for Cl^- and −61.5 kJ mol^{-1} for Br^-, suggesting a weaker ion–water interaction for chloride than for bromide. However, it should be stressed that the structural properties obtained from those all-electron basis sets calculations are very close to the results obtained with the pseudopotentials (used for ions) which are reported in the next section.

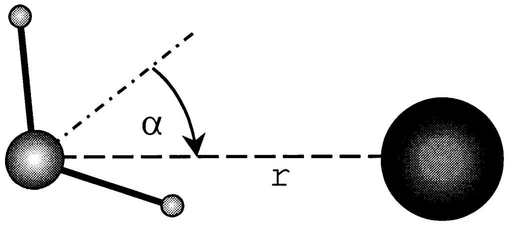

Fig. 1. Starting conformation of the X^-–H_2O systems used in the quantum optimisation calculations.

Besides the HF level, some test calculations including correlation effects were done (at the CCSD(T) level, using again the 6-31G**, the 6-31 + G** and the 6-31 + + G** basis sets for both ion and water), but the improvement in the results did not justify the amount of extra computational cost needed for the construction of the ion–water potentials.

For the two smallest ions, which seem to be the most problematic cases, the water–ion interaction energies found at this level range from −104.5 to −170.2 kJ mol^{-1} for F^- and from −60.8 to −65.4 kJ mol^{-1} for Cl^-. As can be seen, all values computed using the CCSD(T) method overestimate the interaction energies and further corrections would be needed. At the same time, other parameters such as structural parameters as well as charges on the ions obtained with this method are very close to those reported below (see Table 1).

2.2. (b) Results

In Table 1 the results obtained from the optimisation at the HF level with the three different basis sets, (A), (B) and (C), described above, are presented. For each case, the optimal ion–oxygen, $r_{X\text{–}O}$, and ion–hydrogens, $r_{X\text{–}H2}$, and $r_{X\text{–}H2}$, distances, the tilt angle, α, the charge on the ion $Q(X)$ at the optimal conformation and the interaction energy ΔE with and without CP correction are given.

The optimal conformation is found for all ions to be asymmetric, with one hydrogen of the water molecule closer to the ion. The optimal value of α is non-zero for all ions, even for the larger ones. A comparison of the results obtained for the same ion but with different basis sets shows relatively small changes in this property, the largest fluctuation being of ca. 6° for iodide. Similarly, small fluctuations can be observed in the ion–oxygen and ion–hydrogen distances and in the estimates of the charge on the ion at the optimal conformation. The energy values are usually bigger than those reported from experiment. It should be stressed that most combinations of methods and basis sets tested were found to overestimate the experimental energies (sometimes even when corrected for the BSSE), especially in the fluoride case.

A similar effect was reported in a recent work of Kuznetsov [6], where comparative studies using different basis sets for the halide ions and the water molecule were also performed. In that work the structure of the water molecule was in addition optimised. However, the same overestimation of the energy values, as shown in Table 1, was found there mainly for F^- and Cl^-. At the same time, the results obtained in that work for the two larger ions are much closer to the experimental values.

Table 1
Geometrical and energetic properties [a] of the interaction of halide ions with water obtained from the optimisation of the $r_{X\text{–}O}$ distances and α angle with different water basis sets [b,c]

Ion	Basis set type	$r_{X\text{–}H1}$	$r_{X\text{–}O}$	$r_{X\text{–}H2}$	α	$Q(X)$	$-\Delta E_{as}$	$-\Delta E_{as}(CP)$
F^-	(A)	1.591	2.539	2.841	46.1	−0.901	119.0	102.1
	(B)	1.584	2.537	2.865	47.9	−0.897	113.8	96.5
	(C)	1.562	2.516	2.858	48.8	−0.882	119.7	100.4
	Exp. [d]							97.5
Cl^-	(A)	2.294	3.213	3.367	38.7	−0.919	69.6	58.0
	(B)	2.287	3.223	3.429	41.9	−0.917	65.0	54.1
	(C)	2.264	3.203	3.423	42.8	−0.906	67.3	55.8
	Exp. [d]							54.8
Br^-	(A)	2.561	3.462	3.554	35.4	−0.940	55.6	47.7
	(B)	2.552	3.474	3.624	39.0	−0.938	51.2	43.8
	(C)	2.532	3.458	3.622	39.8	−0.929	52.6	44.9
	Exp. [d]							52.7
I^-	(A)	2.939	3.775	3.759	28.8	−0.964	42.9	39.9
	(B)	2.915	3.804	3.849	33.3	−0.963	38.8	34.6
	(C)	2.890	3.788	3.858	34.7	−0.958	39.4	35.4
	Exp. [d]							42.7

[a] Distances in (Å), angles in (°), charges in (a.u.) and energies in (kJ mol^{-1}).
[b] The water basis sets tested are: (A) 6-31G*, (B) 6-31G(2D), (C) 6-31G(3D).
[c] The ΔE(CP) values are the BSSE corrected optimal energies.
[d] Ion–water experimental energies taken from Ref. [46].

A comparison of the geometric properties of the X^-–H_2O systems obtained in the present study, using a rigid water molecule, with those of Kuznetsov suggests that a modification of the water geometry has a rather minor influence on the other structural parameters of the ion–water system. The largest differences between ion–oxygen distances reported here and the ones of Kuznetsov's work are observed for fluoride; for the three other ions this property is in very good agreement.

The values presented here can additionally be compared with other quantum calculations of the interaction of halide ions with water [6,9]. The ion–oxygen distances shown in Table 1 agree very well with the results of Zhan et al. [9]. The $r_{X\text{–}O}$ values, which can be easily calculated from the data given in this paper, are 2.56, 3.21, 3.40 and 3.67 Å for fluoride, chloride, bromide and iodide, respectively. Although in this latter work, as in the work of Kuznetsov mentioned above, the geometry of the water molecule was optimised, some similarities can be found between those published results and the values of $r_{X\text{–}H1}$ and the α angle listed in Table 1. The latter property computed from reported data [9] is found to be of 45.9, 38.2, 37.5 and 23.4° for F^-, Cl,$^-$ Br^- and I^-, respectively. Similar estimates of this angle for the X^-–H_2O systems were found in the work of Kuznetsov [6]. Thus, the structural results shown in Table 1, obtained with a rigid model of water, indeed agree well with those reported in this latter work. Also the Mulliken charge on the ions in the optimal conformation is in good agreement with both mentioned works, being almost constant, slightly increasing when going from fluoride to iodide.

The largest differences between results shown in Table 1 and those previously reported, are the ion–water interaction energy values. As mentioned above, the basis sets were chosen here so that experimental values for the optimal ion–water conformation [46,48] are reproduced, a somewhat difficult task for chloride. In fact, the measured interaction energy of the Cl^-–H_2O system was reported to range from −54.8 [46] to −62.3 kJ mol^{-1} [52]. In our studies the reference experimental energy values were taken from the work of Arshadi et al. [46], where a comparative study of the four halide ions interacting with water was performed.

The combinations of basis sets that closest reproduce the experimental data have been used for the construction of the potential energy surface for each ion. The basis sets selected are the following: (B) for fluoride and chloride, (C) for bromide and (A) for iodide.

For the two smallest ions CP correction is necessary to achieve an agreement between calculated and experimental energy values. In Table 2 the results obtained from the quantum calculations with the chosen basis sets are presented for the symmetric orientation of the water molecule towards the ion, i.e. with an angle α (see Fig. 1) equal to 0°. In this orientation both hydrogens are at the same $r_{X\text{–}H}$ distance from the ion. This ion–

hydrogen distance as well as the ion–oxygen distances, r_{X-O}, the charge on the ion, $Q(X)$, and the interaction energy in this conformation, ΔE_s, are listed in Table 2. The last column of this table contains the differences between energy minima for the optimal (asymmetrical) and the symmetrical conformations of the ion–water system obtained.

When the geometric properties listed in Table 2 are compared with those obtained with the same basis sets for the asymmetric conformation, a systematic increase of the smallest ion–hydrogen distance is seen. This is accompanied by a very small change in the ion–oxygen distance, which increases significantly only for the fluoride–water system, and remains almost unchanged for the three larger ions. The distances presented here are somewhat larger than those reported from other quantum calculations for this conformation [6] which is probably associated with a weaker interaction energy found for the symmetric conformation in the present calculations. The energetic difference between the optimal and symmetric configurations for the four ions shown in Table 2 is somewhat larger than that reported in previous works, especially for fluoride and chloride. This property may be seen as a parameter describing qualitatively the energetic changes in the systems when some reorientation of water molecules around the ion occurs in small gas-phase clusters or in the liquid solution.

3. A new ion–water potential

To construct the potential energy surface of the halide ion–water interaction, a set of additional HF calculations has been performed using the basis sets selected in the previous section. For each ion–water case, eight different orientations of the water monomer towards the ion have been studied and the interaction energies have been computed at various distances, giving a total number of about 150–175 points, depending on the ion. In these calculations the attractive orientations (in which the water molecule has the hydrogens pointing towards the ion) have been favoured, the most stable being asymmetric as described in the previous section (see Fig. 1 and Table 1). As mentioned already, for the four ions, the calculated energy minima for the preferred orientations of water are in agreement with the experimental data of Arshadi et al. [46].

A new potential has been constructed based on the function proposed by Nguyen et al. [41] with an additional ion–oxygen exponential term. This term makes the asymmetric configuration more stable than the symmetric one and reproduces the energetic difference between these structures. The final form of this new potential is:

$$V_{X-W} = V_{X-O} + V_{X-H1} + V_{X-H2} \tag{1}$$

where:

$$V_{X-O} = \frac{A_1}{r_{X-O}} + \frac{A_2}{r_{X-O}^2} f_{or} + A_3 \exp(-A_4 r_{X-O})$$

$$V_{X-H1} = \frac{A_5}{r_{X-H1}} + \frac{A_6}{r_{X-H1}^2} + A_7 \exp(-A_8 r_{X-H1})$$

$$V_{X-H2} = \frac{A_5}{r_{X-H2}} + \frac{A_6}{r_{X-H2}^2} + A_7 \exp(-A_8 r_{X-H2})$$

$$f_{or} = \exp(-A_9 |r_{X-H1} - r_{X-H2}|) \tag{2}$$

The parameters $A_1, \ldots, A_9$ were obtained by fitting the V_{XW} function to the quantum energy points. These parameters are given in Table 3 for each ion. The good quality of the fittings can be observed in Fig. 2, where the quantum interaction energies for the optimal ion–water dimer conformations are plotted against those predicted by the V_{XW} potential. It should be stressed that the pair potential proposed in this work describes the change of the ion–water interaction energy when the H_2O monomer takes less preferred orientations in a remarkable agreement with the quantum points. The behaviour of this potential for those less stable orientations is discussed in detail in our work on the specific adsorption of the halide ions on the Cu(100) surface (Figure 4 in Ref. [66]).

This potential, together with the TIP4P potential [74] for the water molecules, has been used in all simulations described below. The TIP4P potential has been

Table 2
Geometrical and energetic properties [a] obtained with the chosen basis sets [b] for the symmetrical configuration of the X^-–(H_2O) complexes

Ion	Basis set	r_{X-H}	r_{X-O}	$Q(X)$	$-\Delta E_s$	$-(\Delta E_{as} - \Delta E_s)$
F^-	(B_{CP})	2.20	2.65	−0.944	63.3	33.2
Cl^-	(B_{CP})	2.77	3.25	−0.950	43.9	10.2
Br^-	(C)	2.99	3.48	−0.953	47.8	4.8
I^-	(A)	3.25	3.75	−0.945	42.0	0.9

[a] Distances in (Å), angles in (°), charges in (a.u.) and energies in (kJ mol^{-1}).

[b] Same notation for the basis sets as the one used in Table 1.

Table 3
Parameters of the V_{XW} potential for the interaction of halide ions with water (energies in (a.u.) when distances are in (Å))

Parameters	F^-	Cl^-	Br^-	I^-
A_1	0.2681867	0.2896071	0.3651185	0.3905185
A_2	0.1258666	0.1240294	0.1105481	0.1568753
A_3	175.2743391	275.1023705	931.3769637	3955.7403573
A_4	4.0248556	3.5991401	3.99244237	4.5426120
A_5	−0.1306078	−0.1391805	−0.1745202	−0.1895202
A_6	−0.0732078	−0.0838705	−0.1028106	−0.1093375
A_7	5.0219748	4.5382929	3.3018965	4.8860518
A_8	4.0063619	2.9201882	2.3927183	2.2870791
A_9	0.6742457	0.6371453	0.3621453	0.2301453

used in many simulations of processes occurring in aqueous solutions and has proved to describe sufficiently well the properties of bulk water.

4. Gas-phase formation of $X^-(H_2O)_n$ clusters

4.1. (a) Method

In this work, the gas-phase reactions:

$$X^-(H_2O)_{n-1} + H_2O(\text{vapour}) \rightarrow X^-(H_2O)_n \tag{3}$$

where X=F, Cl, Br, I and $n = 1, 2, ..., 10$, have been investigated by the MC method. Thermodynamic properties as well as structural data for the above $X^-(H_2O)_n$ clusters have been studied.

Assuming ideal gas behaviour for the water vapour, the change in enthalpy, $\Delta H_{n-1,n}$, was obtained from:

$$\Delta H_{n-1,n} = \Delta E_{n-1,n} - kT \tag{4}$$

where $\Delta E_{n-1,n}$ stands for the change in internal energy. This has been calculated as the difference between the average energies of the clusters with n and $n-1$ water molecules:

$$\Delta E_{n-1,n} = \langle E_n \rangle - \langle E_{n-1,n} \rangle \tag{5}$$

The energy averages $\langle E_n \rangle$ and $\langle E_{n-1,n} \rangle$ have been obtained directly in conventional MC simulations on the (N, V, T) ensemble at 298 K. In these simulations, the halide ion and the n water molecules surrounding it have been placed in the centre of a box of dimensions 18 × 18 × 18 Å. The simulations have been made according to the Metropolis algorithm and 1×10^6 configurations have been generated for statistical equilibration and 2×10^6 for averaging.

In the same way, the Gibbs free energy $\Delta G_{n-1,n}$ of Eq. (3) has been computed in terms of the Helmholtz free-energy $\Delta A_{n-1,n}$ using the relation:

$$\Delta G_{n-1,n} = \Delta A_{n-1,n} - kT \tag{6}$$

for the standard state of 298 K and 1 atm.

$\Delta A_{n-1,n}$, however, can only be computed by resorting to non-conventional MC simulations and, in this case, the thermodynamic integration method was applied according to the Mruzik et al. approach [13]. In this approach, the potential energy of the cluster is redefined in terms of a coupling parameter λ:

$$U(\lambda) = (1-\lambda)^x U_{n-1} + \lambda^x (U_{n-1} + U_{H_2O}) \tag{7}$$

where $0 < \lambda < 1$, U_{H_2O} is the potential energy of the water molecule (monomer) that is being added to the cluster with $n-1$ water molecules, U_{n-1} is the potential energy of the cluster with $n-1$ water molecules. The coupling parameter λ provides a way of introducing the water monomer into the cluster with $n-1$ water molecules. In fact, when $\lambda = 1$, the monomer is indistinguishable from all the other $n-1$ water molecules, and $U(\lambda = 1) = U_n$. As $\lambda \rightarrow 0$, the monomer becomes effectively invisible to all other particles, and $U(\lambda = 0) = U_{n-1}$. Notice also that if parameter x is equal to 1 in Eq. (7), the formula describes the potential energy of

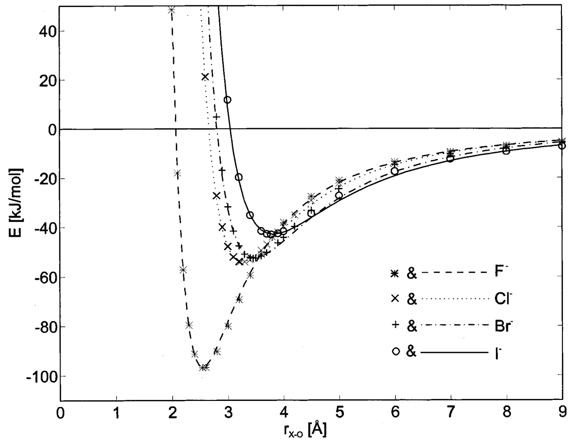

Fig. 2. Interaction energies of the X^-–H_2O systems as functions of the ion–oxygen distance. The points correspond to the quantum calculated energies and the lines to the proposed V_{XW} potential.

Table 4
Calculated and experimental enthalpies $-\Delta H_{n-1,n}$ (kJ mol^{-1}) for the gas-phase formation of X^-–$(H_2O)_n$ clusters (X=F, Cl, Br, I)

$n-1,n$	F^-		Cl^-		Br^-		I^-	
	$-\Delta H_{calc}$	$-\Delta H_{exp}$	$-\Delta H_{calc}$	$-\Delta H_{exp}$	$-\Delta H_{calc}$	$-\Delta H_{exp}$	$-\Delta H_{calc}$	$-\Delta H_{exp}$
0,1	96.2	97.5	53.1	54.8	53.6	52.7	42.4	42.7
1,2	91.7	69.5	53.1	53.1	53.5	51.5	42.2	41.0
2,3	86.9	57.3	52.1	49.0	53.5	48.1	43.8	39.3
3,4	81.4	56.5	50.3	46.4	53.0	45.6	44.4	
4,5	75.3	55.6	50.8		53.1		38.7	
5,6	65.6		47.1		50.1		39.3	
6,7	55.1		46.0		46.6		47.7	
7,8	54.1		46.2		50.7		35.9	
8,9	51.3		47.0		48.9		46.4	
9,10	50.4		42.7		43.9		31.5	

the cluster as a linear function of λ, but this causes some numerical problems related to the sudden increase in the $U(\lambda)$ values when $\lambda \to 0$. In fact, a more convenient way of avoiding numerical integration problems in free-energy calculations of this type is to use a nonlinear λ dependence for the potential energy ($x > 1$). In the present case, x was set equal to 4 as suggested by Mezei [75]. Anyway, the efficiency of the two (linear versus nonlinear) methods has been tested here. It was found that the results obtained with both methods are very close, therefore only those obtained using the nonlinear method are shown in this work.

In addition, parameter λ was made to change nonlinearly from one simulation (window) to another according to the equation [76]:

$$\lambda_{N_w+1} = \frac{1}{2}\left(1 + \tanh\left(\left(\frac{-N}{2} + N_w\right)W_0\right)\right) \tag{8}$$

where N_w is the window number ($N_w = 0, \ldots, N-1$), N is the total number of windows, this being 200 in the present study, and $W_0[=(0.125N)^{-1}]$ is a constant value. This function results in much smaller steps of λ near the edges than in the middle region, which additionally ensures a smooth transformation of the system from the $X^-(H_2O)_{n-1}$ stage to the $X^-(H_2O)_n$ one. In each window a canonical average of the potential energy of the water molecule, $\langle U(\lambda)\rangle$, has been obtained and a total number of 1×10^6 configurations has been generated. The first half of these configurations was used for equilibrating the system and statistical averages were based upon the second half.

During the course of the simulations, the n water molecules were restricted inside a spherical constrained volume (V_c) centred on the ion. With this restriction, the change in Helmholtz free energy, $A_{n-1,n}$, is then given by:

$$\Delta A_{n-1,n} = \int_0^1 U(\lambda)\mathrm{d}\lambda + kT\ln(n) - \int_{V_{1\ \mathrm{atm}}}^{V_c} p\,\mathrm{d}V \tag{9}$$

where $V_{1\ \mathrm{atm}}$ is the constraining volume for a standard state of 298 K and 1 atm. The $p\,\mathrm{d}V$ term in this equation describes the work of expanding the constraining volume V_c until the unattached H_2O monomer is at a pressure of 1 atm. In the present study, the radius of the constraining volume V_c was fixed at 20 Å.

Finally, with the $\Delta G_{n-1,n}$ and $\Delta H_{n-1,n}$ values, the change in entropy, $\Delta S_{n-1,n}$, for each cluster may also be calculated according to the formula:

$$\Delta S_{n-1,n} = (\Delta H_{n-1,n} - \Delta G_{n-1,n})/T \tag{10}$$

4.2. (b) Results

The studies of the gas-phase formation of $X^-(H_2O)_n$ clusters, as described in the last section, can be an important test for the ion–water potentials used in simulations. In Table 4, the calculated values of the enthalpy changes $\Delta H_{n-1,n}$ are shown together with the experimental data available for the four halide ions. Typically, the calculated enthalpies are very close to the experimental values for $n = 1$ and become overestimated for $n = 2$. It may be said that for n up to ca. 4–5 the $\Delta H_{n-1,n}$ estimates are almost constant and the decrease of their values appears for larger n than it is predicted from experiment. For $n \geq 6$ some asymptotic behaviour can be observed in Table 4, as the $\Delta H_{n-1,n}$ values tend to the values suggested by the experimental measurements for small clusters.

It should be noticed that for iodide the oscillations of enthalpy values are found to be quite large even for n close to 10. This ion is characterised by a relatively weak interaction with water, being of similar magnitude to the strength of hydrogen bonds between waters. Thus, as the properties of the hydration shell of this ion result from a balance of similar forces they may be more sensitive to the type of potential used than it is expected for the other ions. In fact, a test was performed with another form of the ion–water potential fitted to the same quantum points as described in Section 3. The results obtained with this potential were almost the same for the three larger ions, but very different for iodide. Nevertheless, the large fluctuations in the values of $\Delta H_{n-1,n}$ obtained for larger n, as those observed in Table 4, were the common feature of both potentials tested.

In most earlier theoretical studies of the gas-phase formation of the X^-–$(H_2O)_n$ clusters, only relatively small structures have been investigated. It should be noticed that the other calculated enthalpies do not show a similarly clear trend. However, it should be said that the present enthalpies correlate to the experimental data as well as those previously obtained with more refined models [14–21]. The reported data suggest that a better fit to the experimental enthalpy values for the whole range of n can only be achieved by introducing many-body effects into the model.

The Gibbs free-energies $\Delta G_{n-1,n}$ for the gas-phase formation of the X^-–$(H_2O)_n$ clusters, computed according to Eq. (6), are shown in Table 5. For comparison, the experimental values are also shown. The $\Delta G_{n-1,n}$ values have been calculated only in the forward direction $\lambda = 0 \rightarrow \lambda = 1$ (formation of the cluster with n water molecules), using a nonlinear λ-dependence for the potential energy. In fact, the tests made for some chosen cases showed no particular difference between the results in both directions (forward: $\lambda = 0 \rightarrow \lambda = 1$ and backwards: $\lambda = 1 \rightarrow \lambda = 0$) or for the two approaches (linear and nonlinear). Nevertheless, the nonlinear λ-dependence should be preferred as the errors were found to be smaller by a factor of at least two.

The absolute values of the free energies obtained from the MC simulations, when compared with the experimental data, exhibit similar tendencies as found for the enthalpies. This is, for $n = 1$, they are very close to the experimental estimates and for $n > 1$ they overestimate them. For chloride, bromide and iodide and for $n \rightarrow 10$ the computed $\Delta G_{n-1,n}$ values tend asymptotically to a similar value (≈ 9 kJ mol^{-1}) which is close to the value of condensation of the water vapour [77], while still much larger values are noted for fluoride. This latter ion is, in general, the most difficult one to properly describe using theoretical methods. The peculiar behaviour of the experimental $\Delta G_{n-1,n}$ estimates, i.e. the decrease of their absolute values up to $n = 4$ and then their increase, is difficult to be reconstructed. Some slight overestimation of the free energy changes for bromide in relation to chloride, should be noticed at the same time. This effect is not unexpected taking into account that the analytical potentials constructed for these ions have similar energy minima and mostly differ in terms of steric properties. The results of the present work are in a qualitative way similar to those shown in the paper of Mruzik et al. [13] where the stepwise free energies of the ions solvation have been calculated for fluoride and chloride, but only for clusters with n not greater than 6.

In Table 6 the entropy values as calculated from Eq. (10) are shown together with the experimentally reported entropy estimates. Of course, the results presented here are obtained indirectly, from two relatively large values of $\Delta H_{n-1,n}$ and of $\Delta G_{n-1,n}$, and so their estimates may be charged by a quite large error. Nevertheless, their good agreement with experimental data should be noticed from the Table 6, especially for larger ions.

Table 5

Calculated and experimental Gibbs free energies $-\Delta G_{n-1,n}$ (kJ mol^{-1}) for the gas-phase formation of $X^-(H_2O)_n$ clusters (X = F, Cl, Br, I)

$n-1,n$	F^-		Cl^-		Br^-		I^-	
	$-\Delta G_{calc}$	$-\Delta G_{exp}$	$-\Delta G_{calc}$	$-\Delta G_{exp}$	$-\Delta G_{calc}$	$-\Delta G_{exp}$	$-\Delta G_{calc}$	$-\Delta G_{exp}$
0,1	68.0	75.7	29.7	34.3	31.2	29.3	21.5	22.6
1,2	61.3	46.0	26.7	27.2	27.5	23.0	18.8	17.6
2,3	54.0	31.8	23.1	18.8	24.3	17.2	16.2	13.0
3,4	47.3	23.0	20.8	14.2	22.2	12.1	14.9	
4,5	38.4	29.7	18.7		19.3		12.9	
5,6	30.3		16.2		18.1		12.3	
6,7	22.1		13.4		16.1		11.0	
7,8	18.5		13.3		14.8		10.6	
8,9	16.3		12.7		14.0		10.3	
9,10	17.7		9.6		12.3		9.1	

Table 6
Calculated and experimental entropies $-\Delta S_{n-1,n}$ (cal mol^{-1} K^{-1}) for the gas-phase formation of $X^-(H_2O)_n$ clusters (X = F, Cl, Br, I)

$n-1,n$	F^-		Cl^-		Br^-		I^-	
	$-\Delta S_{calc}$	$-\Delta S_{exp}$	$-\Delta S_{calc}$	$-\Delta S_{exp}$	$-\Delta S_{calc}$	$-\Delta S_{exp}$	$-\Delta S_{calc}$	$-\Delta S_{exp}$
0,1	22.6	17.4	18.8	16.5	17.9	18.4	16.7	16.3
1,2	24.4	18.7	21.1	20.8	20.8	22.9	18.8	19.0
2,3	26.3	20.4	23.3	23.5	23.4	24.8	22.2	21.3
3,4	27.3	36.9	23.7	25.8	24.7	26.8	23.7	
4,5	29.6	30.7	25.8		27.0		20.7	
5,6	28.3		24.8		25.7		21.6	
6,7	26.4		26.2		24.5		28.6	
7,8	28.6		26.4		28.8		20.3	
8,9	28.1		27.5		28.0		29.0	
9,10	26.2		26.5		25.3		18.0	

In order to get a better insight on the cluster structures, MC optimisations at 0 K have been performed for each cluster. Table 7 presents the values of the ion–water and water–water components of the interaction energies calculated per water molecule for the optimised clusters. They can be analysed in conjunction with Figs. 3 and 4, where the structures of the fluoride and iodide optimised clusters are shown as examples.

As can be seen in Figs. 3 and 4, the anion–water clusters rarely adopt symmetric configurations. The final geometry of the cluster is clearly determined by the dominance of one of the two energy components shown in Table 7. Two typical arrangements of the water molecules around the anions can be distinguished in Figs. 3 and 4: the surface (S) structure and the interior (I) structure. The (S) structures are formed when the hydrogen bonding between water molecules dominates the ion–water interactions, thus water molecules organise themselves together on one side of the ion. In the (I) structures the cluster geometry is determined by the stronger ion–water interactions as well as by hydrogen bonding between subgroups of water molecules. In this case the ion is located either between one group of waters and another group or between one group of waters and just one isolated H_2O molecule.

As shown in Figs. 3 and 4, for the small clusters $n=2$–3, the (S) structures are preferred for both ions. For $n=4$ a difference appears between the structures found; the (I) structure is found for fluoride, while the (S) conformation is stabilised for iodide. The changes in water–water and ion–water energies when clusters with three and four water molecules are compared in Table 7 confirm the dominance of the different energy components.

For fluoride the U_{WW} energy becomes suddenly positive for $F^-(H_2O)_4$, exhibiting a sudden repulsion between waters, while for $I^-(H_2O)_4$ this component is more negative than for $I^-(H_2O)_3$. At the same time, the second component, U_{WS}, decreases for fluoride and increases for iodide when clusters with three and four waters are compared. Thus, the (I) structure for fluoride (Fig. 3(d)) is indeed stabilised by the dominance of the ion–water interaction, while an opposite phenomenon, i.e. the dominance of the water–water interaction over the ion–water interaction, occurs for iodide (Fig. 4(d)). A relative decrease of the U_{WW} average energy when going to the next $F^-(H_2O)_5$ cluster, together with an increase of the U_{WS} value, suggests that in this case the surface structure rather than the interior can be expected. Inspection of Fig. 3(e) confirms that the surface geometry is found for this cluster. Although the type of structure of the $X^-(H_2O)_5$ cluster is the same for both ions, namely a (S) type, their geometry differs very significantly.

The spatial properties of the ion are decisive for the conformation adopted by the five water molecules: for the larger iodide it is a quasi regular planar pentagon, while for fluoride, a first shell of four water molecules is somewhat deformed by the fifth water molecule located farther away from the ion. For the larger clusters with $n \geq 6$ there is always a prevalence of (I) type structures and the progressive process of closing the hydration shell around the ion can be observed as n value increases. Analysing the U_{WW} and U_{WS} energy components for chloride and bromide, one may conclude, that the (I) structure appears for bromide when $n=6$, as it was found for iodide. For chloride, the decrease in the U_{WW} energy occurs only for $n=8$, and this deviation from the general trend may suggest that this potential may still be improved. For the other three ions, the

Table 7
Water–water (U_{WW}) and ion–water (U_{WS}) interaction energies per water molecule (kJ mol^{-1}) obtained for the X^-–$(H_2O)_n$ clusters at 0 K

n	F^-		Cl^-		Br^-		I^-	
	U_{WW}	U_{WS}	U_{WW}	U_{WS}	U_{WW}	U_{WS}	U_{WW}	U_{WS}
1	0.0	−97.6	0.0	−54.6	0.0	−54.9	0.0	−43.7
2	−1.3	−96.5	−5.7	−53.5	−6.3	−53.7	−7.1	−42.3
3	−3.4	−95.0	−7.2	−52.6	−13.3	−52.0	−9.7	−41.2
4	1.3	−95.2	−7.3	−51.8	−15.5	−50.6	−17.7	−38.8
5	−7.1	−81.1	−7.7	−51.0	−16.4	−46.9	−16.7	−37.9
6	−2.5	−85.1	−14.1	−46.5	−13.8	−46.9	−10.4	−38.4
7	−0.3	−85.6	−15.8	−44.0	−18.0	−43.8	−16.5	−35.1
8	−2.5	−79.5	−11.3	−45.3	−19.5	−39.6	−12.4	−38.3
9	−5.7	−74.2	−17.3	−39.3	−13.7	−44.7	−14.4	−35.9
10	−6.5	−69.2	−16.2	−39.9	−19.3	−39.4	−17.7	−32.4

transition from the (S) to the (I) structure is found in the present work to occur for clusters with four to six water molecules, depending on the type of ion.

The finding that the (S) → (I) transition occurs in the range of n between 4 for fluoride and around 6 for larger ions, goes counter to the conclusions of earlier MD studies [19–21,23] where the (S) structures have been suggested to be dominant for $n \leq 15$. However, our results do agree very well with that reported from recent quantum calculations [2–5], where the structural properties of the $X^-(H_2O)_n$ clusters ($n = 1, ..., 6$) have been studied by ab initio calculations.

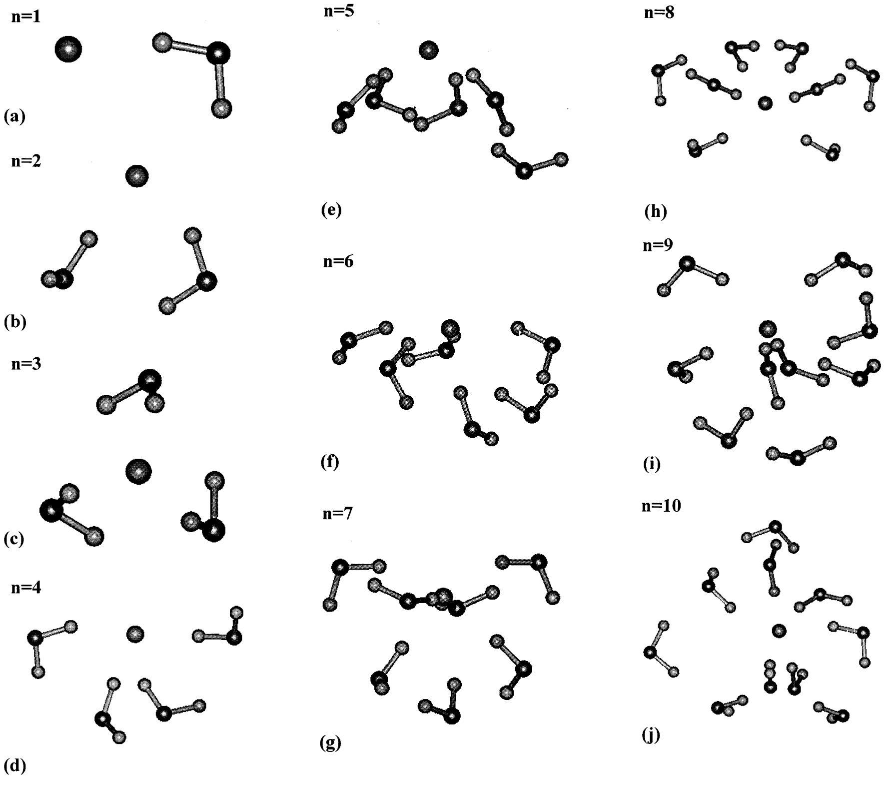

Fig. 3. (a–j) Optimised structures found for the $F^-(H_2O)_n$ clusters ($n = 1, ..., 10$) at 0 K.

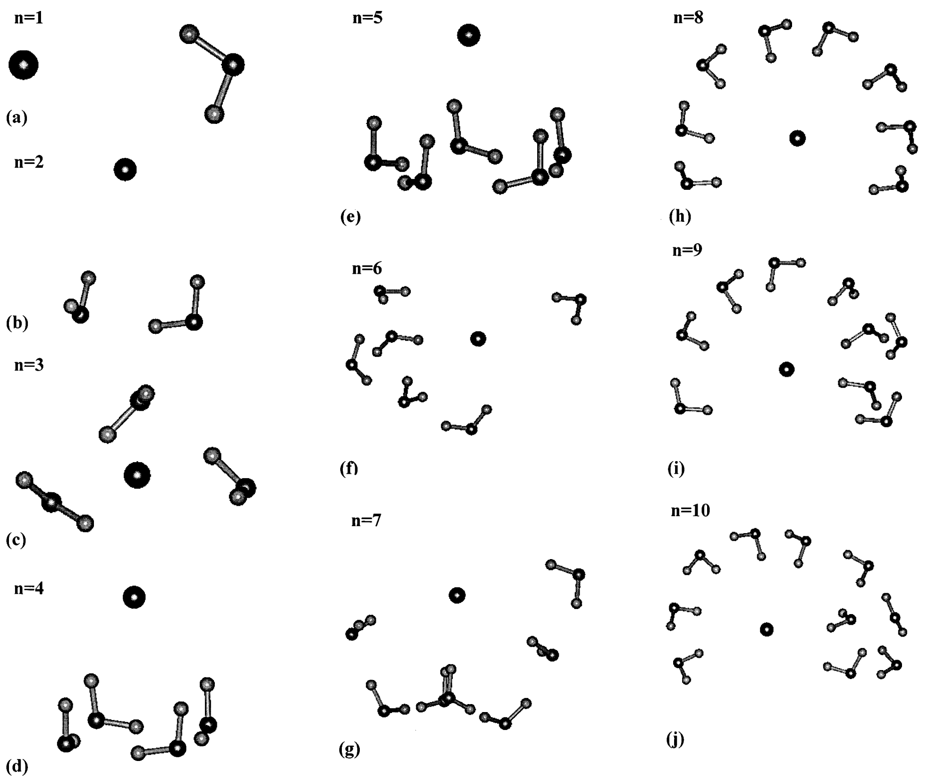

Fig. 4. (a–j) Optimised structures found for the $I^-(H_2O)_n$ clusters ($n = 1, ..., 10$) at 0 K.

5. Halide ions in aqueous solution

5.1. (a) Method

The studies of the aqueous solutions of halide ions have been done by means of conventional MC simulations on the (N, V, T) ensemble at a standard temperature of 298 K. For each ion, diluted solutions were modelled by the X^-–$(H_2O)_{196}$ system in a cubic box with side lengths of 18.02 Å. At these conditions a density of about 1 g cm^{-3} is achieved for the solutions. The simulations have been performed according to the Metropolis algorithm and periodic boundary conditions were applied under the minimal image convention. About 6×10^6 configurations have been used for statistical equilibration and sampling.

5.2. (b) Results

The structure of the solution around each ion was analysed in terms of RDFs as well as running coordination numbers. The results of these calculations are presented in Fig. 5. Due to the role of hydrogen in the bonding of water to the anion, the first hydration shell of the halides is clearly defined by the $\mathrm{RDF}_{X\text{–}H}$ but only moderately by the $\mathrm{RDF}_{X\text{–}O}$, this being especially true for the larger anions. The distribution of oxygens around the ions is only well defined for fluoride, as for the other ions it exhibits a rather broadened behaviour beyond the first maximum of $\mathrm{RDF}_{X\text{–}O}$. This might suggest that the first hydration shell has a much more diffuse character for the larger ions than it has for fluoride. As was mentioned before, for chloride, bromide and iodide, the ion–water interaction is relatively weak when compared with the strength of hydrogen bonding. Given this rather unclear shape of the $\mathrm{RDF}_{X\text{–}O}$, the coordination number for all halide ions has been obtained from the integration of the $\mathrm{RDF}_{X\text{–}H}$ functions.

It can be seen that the computed structural properties, such as the radius of the first hydration shell and the coordination number of the ions are in quite good agreement with experimental data considering the range of uncertainties of this data, and the fact that the model proposed here is relatively simple and does not include many-body interactions. The overestimation of the coordination number of fluoride is not unusual in statistical models, as can be seen by inspection of the results obtained here and in earlier studies which are listed in Table 8. In fact, for chloride [18], it has been shown that the inclusion of three-body forces is necessary to obtain a coordination number in better agreement with experiment as an overestimation was obtained when only two-body potentials were used.

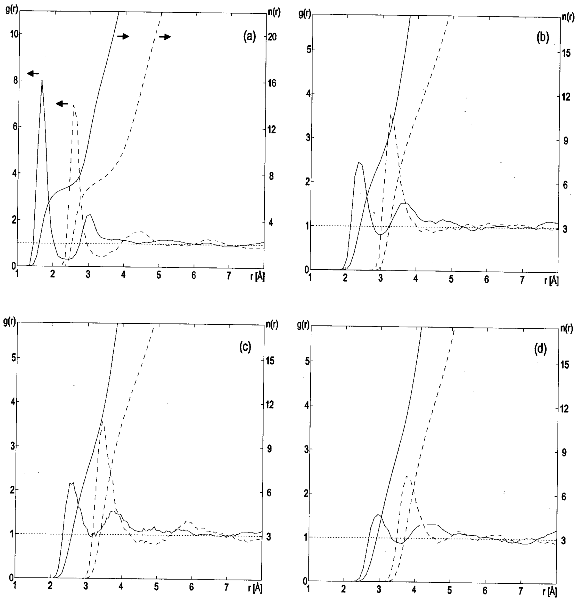

Fig. 5. Radial hydrogen (solid lines) and oxygen (dashed lines) distribution functions $g(r)$ and running coordination numbers $n(r)$ of the four halide ions in aqueous solution at 298 K: (a) F^-, (b) Cl^-, (c) Br^-, (d) I^-. Arrows in (a) show to which scale the curve should be related.

The RDFs' results presented here are qualitatively similar to those shown in a very recent work of Toth [45], where the properties of the four halide ions in solution have been investigated using the TIP4P potential for the water–water interactions. For all halide ions, the orientation of waters in the first hydration shell has also been found to have one hydrogen closer to the ion. The coordination numbers obtained here are slightly larger than n_{H_2O} values reported in that paper, except for iodide for which a larger coordination number was found in the work of Toth. Notice that in this work the ion–water potentials have been also parameterised by fitting to quantum energy points, but it should be stressed that these quantum results strongly underestimated the X^-–H_2O interaction energy, especially for fluoride. This effect is also seen in the computed solvation energies for the three larger ions, which appear to be underestimated in comparison with the experimental values.

In Table 9, the solvation enthalpies for the four halide ions in aqueous solution obtained in the present work are shown. These enthalpies have been computed as:

$$\Delta E_{sol} = E_{X\text{–}W} + E_{W\text{–}W} - E^{*}_{W\text{–}W} \qquad (11)$$

where $E_{X\text{–}W}$ and $E_{W\text{–}W}$ stand, respectively, for the ion–water and water–water interaction energies of the solution and $E^{*}_{W\text{–}W}$ for the water–water interaction energy of pure water.

Table 8
Positions of the maxima of the radial oxygen (rO) and hydrogens (rH_1 and rH_2) distribution functions $g(r)$ obtained for the four halide ions in aqueous solution at 298 K [a]

Ion	Ref.	rH_1	rO	rH_2	n_{H_2O}
F^-	[33]		2.60		4.09
	[40]	1.73	2.67	3.07	5.8
	[41]	1.60	2.64	2.88	6
	[34]	1.65	2.60		6.2
	[42]	1.65	2.64		6.8
	[78]	1.35	2.75		7.0
	[45]	1.67	2.61		6.0
	This work	1.625	2.575	3.025	6.7
	Exp. [57]				4.5
Cl^-	[32]	2.50	3.20		5.7
	[33]		3.25		8.36
	[40]	2.35	3.29	3.73	7.2
	[41]	2.32	3.28	3.68	7
	[34]	2.25	3.21		7.4
	[42]	2.24	3.22		8.2
	[43]	2.29	3.23		
	[78]	2.00	3.45		11.7
	[45]	2.25	3.19		7.0
	This work	2.325	3.225	3.725	7.5
	Exp. [58]	2.29	3.20		8–8.2
	Exp. [59]	2.25	3.34		5.9
Br^-	[45]	2.45	3.37		7.3
	This work	2.625	3.425	3.775	8.2
	Exp. [60]		3.14–3.43		
I^-	[42]	3.40	3.68		8.7
	[45]	2.77	3.71		9.7
	This work	2.925	3.775	4.125	9.1
	Exp. [60]		3.64–3.76		6 [54]

[a] In the last column the number of water molecules of the first hydration shell of the ion is given. For comparison, the results of other theoretical and experimental works are also shown.

Table 9
Solvation energies ΔE_{solv} (kJ mol^{-1}) obtained from the simulations of halide ions at infinite dilution ($T = 298$ K), for comparison, the results of some experimental hydration enthalpies are also shown

Ion	This work	[61]	[62]	[63]
F^-	620	484	473	518
Cl^-	352	341	340	376
Br^-	345	314	327	345
I^-	296	273	268	300

Comparison of computed values with experimental ones shows a very good agreement between these quantities for the three larger ions, i.e. chloride, bromide and iodide. For fluoride, the calculated solvation enthalpy is overestimated. On the other hand, it can be seen in Table 9 that the uncertainty in experimental data, when different measurements are compared, is relatively large for all ions.

6. Conclusions

Standard HF calculations have been performed for the interaction of halide ions with water. As it is common practice, the basis sets were chosen to best reproduce the experimental values in a consistent way. The results of these calculations confirm that, for the ion–water dimers, the water molecule interacts with the halide ions through hydrogen bonding. Independently of the basis sets used, the optimal conformation is always found to be the asymmetric one, with one hydrogen closer to the halide ion. For all tested basis sets, the tilt angle between the dipole moment and the ion–oxygen vector is larger for fluoride and decreases when going to iodide. For fluoride, the F^-–H–O bond appears to be almost linear. From the comparison of results of the present study and those reported in literature it appears that no significant errors are introduced in the calculations when using a rigid model for the water molecule. This is also true for the basis sets giving the best estimates in relation to the experimentally known properties.

The calculations performed with the chosen basis sets showed that for the X^-–H_2O systems there exists a significant decrease in the interaction energy when the water is reoriented from the optimal asymmetric position to the symmetric one (orientation in which the two hydrogens are pointing towards the ion). This energetic difference has been found to be especially large for fluoride. This may be expected to play an important role in processes where the structure of the first hydration shell of the ion is significantly changed, like in the specific adsorption of ions from the solution onto the metal surface [66]. In fact, a detailed knowledge and understanding of all subtle effects of ions under special conditions in aqueous environment is of great importance for the studies of the complex adsorption process. The ion cannot be contact adsorbed on the surface without making some significant modification of its closest hydration shell, at least in the direction towards the surface. This may be associated with a strong reorientation of waters and even with the removal of some of them from the first hydration shell, and so it would be very important for the energetic description of the adsorption phenomenon.

The new potential proposed in this work for the description of the interactions of halide ions with water has been used in MC simulations of the X^-–$(H_2O)_n$ systems. It has been shown to give good quality results in the simulations of halide ions in the gas-phase clusters and in solution, considering that this simple model does not include many-body effects. The thermodynamic and structural properties of the $X^-(H_2O)_n$ systems are reproduced at a similar level of quality as in some earlier theoretical studies using pair potentials. In fact, the enthalpy and the free energy computed for the gas-phase formation of small clusters exhibit tendencies equivalent to those reported in other theoretical works. In some cases, however, a significant improvement in the results has been achieved in the present work. Unlike earlier simulations performed for the small X^- $(H_2O)_n$ clusters, the transition from the (S) structure to the (I) structure was found to occur already for small n (from 4 to 6). This is in very good agreement with the results of recent published quantum studies (that include many-body effects), using extended basis sets [2–5]. In those studies, it was suggested that the (S) to (I) transition should occur at $n = 4–5$ for fluoride, and at n around 6 for larger ions. The same trend and the same n values were found on the present simulations. With respect to the ions in liquid phase, the structural properties of their aqueous environment have been found to be in good agreement with those reported experimentally. Very good results are obtained using the present new potential for estimating solvation energies, when computed values are compared with the experimental data, especially for the three larger ions. Anyway, it should be said that the experimental determination of the properties of halide ions in aqueous solution depends strongly on the models assumed. The list of the structural and thermodynamical experimental values presented here, though incomplete, clearly shows how large it is the margin of uncertainty of the experimental data. The potential used in this work was chosen to follow one set of proposed experimental values, although other options certainly exist. This is an assumption of the present work that should be taken into account.

Acknowledgements

The authors thank Professor S. Romanowski of the University of Lodz (Poland) for discussions that originated this project. The financial support of Praxis XXI through project PRAXIS/PCEX/C/QUI/61/96 is acknowledged. A.I. thanks PRAXIS XXI for a doctoral scholarship.

References

[1] J.E. Del Bene, J. Phys. Chem. 92 (1988) 2874.

[2] J.E. Combariza, N.R. Kestner, J. Jortner, Chem. Phys. Lett. 20 (1993) 423.

[3] J.E. Combariza, N.R. Kestner, J. Phys. Chem. 98 (1994) 3513.
[4] J.E. Combariza, N.R. Kestner, J. Jortner, J. Chem. Phys. 100 (1994) 2851.
[5] J.E. Combariza, N.R. Kestner, J. Jortner, Chem. Phys. Lett. 221 (1994) 156.
[6] An.M. Kuznetsov, Chem. Phys. 179 (1994) 47.
[7] S.S. Xantheas, T.H. Dunning Jr., J. Phys. Chem. 98 (1994) 13489.
[8] S.S. Xantheas, J. Phys. Chem. 100 (1996) 9703.
[9] C.-G. Zhan, S. Iwata, Chem. Phys. Lett. 232 (1995) 72.
[10] J.E. Combariza, N.R. Kestner, J. Phys. Chem. 99 (1995) 2717.
[11] T.P. Lybrand, P.A. Kollman, J. Chem. Phys. 83 (1985) 2923.
[12] H. Kistenmacher, H. Popkie, E. Clementi, J. Chem. Phys. 61 (1974) 799.
[13] M.R. Mruzik, F.F. Abraham, D.E. Schreiber, G.M. Pound, J. Chem. Phys. 64 (1976) 481.
[14] S.-S. Sung, P.C. Jordan, J. Chem. Phys. 85 (1986) 4045.
[15] P. Cieplak, T.P. Lybrand, P.A. Kollman, J. Chem. Phys. 86 (1987) 6393.
[16] S. Lin, P.C. Jordan, J. Chem. Phys. 89 (1988) 7492.
[17] J. Caldwell, L.X. Dang, P.A. Kollman, J. Am. Chem. Soc. 112 (1990) 9144.
[18] L.X. Dang, J.E. Rice, J. Caldwell, P.A. Kollman, J. Am. Chem. Soc. 113 (1991) 2481.
[19] L. Perera, M.L. Berkowitz, J. Chem. Phys. 95 (1991) 1954.
[20] L. Perera, M.L. Berkowitz, J. Chem. Phys. 99 (1993) 4222.
[21] L. Perera, M.L. Berkowitz, J. Chem. Phys. 99 (1993) 4236.
[22] W.L. Jorgensen, D.L. Severance, J. Chem. Phys. 99 (1993) 4233.
[23] L.X. Dang, B.C. Garret, J. Chem. Phys. 99 (1993) 2972.
[24] L. Perera, M.L. Berkowitz, J. Chem. Phys. 100 (1994) 3085.
[25] L.S. Sremaniak, L. Perera, M.L. Berkowitz, Chem. Phys. Lett. 218 (1994) 377.
[26] L.S. Sremaniak, L. Perera, M.L. Berkowitz, J. Phys. Chem. 100 (1996) 1350.
[27] S.J. Stuart, B.J. Berne, J. Phys. Chem. 100 (1996) 11934.
[28] I.-C. Yeh, L. Perera, M.L. Berkowitz, Chem. Phys. Lett. 264 (1997) 31.
[29] E. Clementi, R. Barsotti, Theor. Chim. Acta 43 (1976) 101.
[30] F.T. Marchese, D.L. Beveridge, J. Am. Chem. Soc. 106 (1984) 3713.
[31] B.M. Rode, S.M. Islam, Y. Yongyai, Pure Appl. Chem. 63 (1991) 1725.
[32] M.N.D.S. Cordeiro, R. Cammi, J.A.N.F. Gomes, J. Tomasi, Theor. Chim. Acta 82 (1992) 165.
[33] M. Mezei, D.L. Beveridge, J. Chem. Phys. 74 (1981) 6902.
[34] J. Chandrasekhar, D.C. Spellmeyer, W.L. Jorgensen, J. Am. Chem. Soc. 106 (1984) 903.
[35] K. Heinzinger, Pure Appl. Chem. 57 (1985) 1031.
[36] T. Yamaguchi, H. Ohtaki, E. Spohr, G. Palinkas, K. Heinzinger, Z. Naturforsch. A 41 (1986) 1175.
[37] W. Meier, Ph. Bopp, M.M. Probst, E. Spohr, J.-I. Lin, J. Phys. Chem. 94 (1990) 4672.
[38] I. Benjamin, J. Chem. Phys. 95 (1991) 3698.
[39] D.E. Smith, L.X. Dang, J. Chem. Phys. 100 (1994) 3757.
[40] R.W. Impey, P. Madden, I.R. McDonald, J. Phys. Chem. 87 (1983) 5071.
[41] H.L. Nguyen, S.A. Adelman, J. Chem. Phys. 81 (1984) 4564.
[42] K. Heinzinger, G. Pálinkás, in: R.R. Dogonadze Jr., et al. (Eds.), The Chemical Physics of Solvation, vol. 38A, Elsevier, Amsterdam, 1986, p. 313.
[43] D.G. Bounds, Mol. Phys. 54 (1985) 1335.
[44] M. Kiselev, M. Poxleitner, J. Seitz-Beywl, K. Heinzinger, Z. Naturforsch. A 48 (1993) 806.
[45] G. Tóth, J. Chem. Phys. 105 (1996) 4564.
[46] M. Arshadi, R. Yamdagni, P. Kebarle, J. Phys. Chem. 74 (1970) 1475.
[47] R.G. Keesee, W. Castleman Jr., Chem. Phys. Lett. 74 (1980) 139.
[48] M.A. French, S. Ikuta, P. Kebarle, Can. J. Chem. 60 (1982) 139.
[49] G. Caldwell, P. Kebarle, J. Am. Chem. Soc. 106 (1984) 967.
[50] J.W. Larson, T.B. McMahon, J. Am. Chem. Soc. 106 (1984) 517.
[51] L.W. Sieck, J. Phys. Chem. 89 (1985) 5552.
[52] S. Yamabe, Y. Furumiya, K. Hiraoka, K. Morise, Chem. Phys. Lett. 131 (1986) 261.
[53] K. Hiraoka, S. Mizuse, Chem. Phys. 118 (1987) 457.
[54] G. Markovich, R. Giniger, M. Levin, O. Chesnovsky, J. Chem. Phys. 95 (1991) 9416.
[55] J.E. Enderby, Pure Appl. Chem. 57 (1985) 1025.
[56] J.E. Enderby, S. Cummings, G.J. Herdman, G.W. Neilson, P.S. Salmon, N. Skipper, J. Phys. Chem. 91 (1987) 5851.
[57] D.S. Terekhova, A.I. Ryss, I.V. Radchenko, Zh. Strukt. Khim. 10 (1969) 107.
[58] L. Licheri, G. Piccaluga, G. Pinna, J. Appl. Crystallogr. 6 (1973) 392.
[59] J.R. Newsome, G. Neilson, J.E. Enderby, J. Phys. C 13 (1980) L923.
[60] J.E. Enderby, G.W. Neilson, in: F. Franks (Ed.), Water a Comprehensive Treatise, vol. I, Plenum Press, New York, 1979.
[61] J.O'M. Bockris, A.K.N. Reddy, Modern Electrochemistry, Plenum Press, New York, 1970.
[62] P. Kebarle, in: B.E. Conway, J.O'M. Bockris (Eds.), Modern Aspects of Electrochemistry, Plenum Press, New York, 1974.
[63] Y. Marcus, Ion Solvation, Wiley, New York, 1985.
[64] A. Ignaczak, J.A.N.F. Gomes, Chem. Phys. Lett. 257 (1996) 609.
[65] A. Ignaczak, J.A.N.F. Gomes, J. Electroanal. Chem. 420 (1997) 71.
[66] A. Ignaczak, J.A.N.F. Gomes, S. Romanowski, J. Electroanal. Chem. 450 (1998) 175.
[67] W.R. Wadt, P.J. Hay, J. Chem. Phys. 82 (1985) 284.
[68] T.H. Dunning, P.J. Hay, Modern Theoretical Chemistry, Plenum Press, New York, 1976, pp. 1–28.
[69] W.J. Hehre, R. Ditchfield, J.A. Pople, J. Chem. Phys. 56 (1972) 2257.

[70] M.J. Frisch, J.A. Pople, J.S. Binkley, J. Chem. Phys. 80 (1984) 3265.

[71] T. Clark, J. Chandrasekhar, G.W. Spitznagel, P.V.R. Schleyer, J. Comp. Chem. 4 (1983) 294.

[72] S.F. Boys, F. Bernardi, Mol. Phys. 19 (1970) 553.

[73] (a) Gaussian 92/DFT, Revision F.2, M.J. Frisch, G.W. Trucks, H.B. Schlegel, P.M.W. Gill, B.G. Johnson, M.W. Wong, J.B. Foresman, M.A. Robb, M. Head-Gordon, E.S. Reprogle, R. Gomperts, J.L. Andres, K. Ragchavachari, J.S. Binkley, C. Gonzales, R.L. Martin, D.J. Fox, D.J. DeFrees, J. Baker, J.P. Stewart, J.A. Pople, Gaussian Inc. Pittsburgh, PA, 1993. (b) Gaussian 98, Revision A.3, M.J. Frisch, G.W. Trucks, H.B. Schlegel, G.E. Scuseria, M.A. Robb, J.R. Cheeseman, V.G. Zakrzewski, J.A. Montgomery, Jr., R.E. Stratmann, J.C. Burant, S. Dapprich, J.M. Millam, A.D. Daniels, K.N. Kudin, M.C. Strain, O. Farkas, J. Tomasi, V. Barone, M. Cossi, R. Cammi, B. Mennucci, C. Pomelli, C. Adamo, S. Clifford, J. Ochterski, G.A. Petersson, P.Y. Ayala, Q. Cui, K. Morokuma, D.K. Malick, A.D. Rabuck, K. Raghavachari, J.B. Foresman, J. Cioslowski, J.V. Ortiz, B.B. Stefanov, G. Liu, A. Liashenko, P. Piskorz, I. Komaromi, R. Gomperts, R.L. Martin, D.J. Fox, T. Keith, M.A. Al-Laham, C.Y. Peng, A. Nanayakkara, C. Gonzalez, M. Challacombe, P.M.W. Gill, B. Johnson, W. Chen, M.W. Wong, J.L. Andres, C. Gonzalez, M. Head-Gordon, E.S. Replogle, J.A. Pople, Gaussian, Inc., Pittsburgh PA, 1998.

[74] W.L. Jorgensen, J. Chandrasekhar, J. Madura, R.W. Impey, M.L. Klein, J. Chem. Phys. 79 (1983) 926.

[75] M. Mezei, J. Comp. Chem. 13 (1992) 651.

[76] N. Migliore, G. Corongiu, E. Clementi, G.C. Lie, J. Chem. Phys. 88 (1988) 7766.

[77] I. Prigorgine, R. Defay, Chemical Thermodynamics, Jarrold, Norwich, 1988.

[78] B.M. Pettitt, P.J. Rossky, J. Chem. Phys. 84 (1986) 5836.